Original paper

MULTISOURCE DATA INTEGRATION FOR GROUNDWATER PROSPECTING IN PRECAMBRIAN SHEAR ZONES, ESPÍRITO SANTO STATE (SOUTHEASTERN BRAZIL)

Marcos Eduardo Hartwig[1*], César Augusto Moreira[2] and Marilane Gonzaga de Melo[2]

Received: April 26, 2020; accepted: November 18, 2020; published online: April 1, 2021.

RESUMEN

Las rocas metamórficas Precámbricas en la región sur del estado de Espírito Santo (sureste de Brasil) están interceptadas por zonas de cizallamiento dúctiles y quebradizas / dúctiles sobre las cuales se establecieron pueblos como Guaçuí, Marechal Floriano y Domingos Martins. En los años de 2014 a 2016, el estado de Espírito Santo enfrentó la peor sequía de los últimos 80 años. En situaciones como esa, la única fuente de agua dulce disponible es subterránea. Por lo tanto, el propósito de este estudio fue integrar datos de fuentes múltiples para la prospección y gestión de aguas subterráneas. El área de estudio comprende los sectores centrales de las zonas de cizallamiento Guaçuí y Batatal. La metodología abarca la interpretación de pares estereoscópicos para la identificación de lineamientos estructurales, prospección geofísica (resistividad eléctrica) y trabajos geológicos de campo. Los resultados se validaron tentativamente con los datos de producción de pozos de agua subterránea disponibles. Se estudiaron seis perfiles de resistividad con una longitud total de 2.400 m y se describieron 15 afloramientos. Los resultados mostraron que el marco estructural de las zonas de cizallamiento está hecho predominantemente de lineamientos de orientación NW a NNW y NE a NNE. La familia de orientación NW-NNW está relacionada con la tectónica frágil y la familia de orientación NE-NNE coincide con la trama dúctil Precámbrica de las rocas cristalinas del basamento. Un acuífero poroso superficial relacionado al regolito y a depósitos sedimentarios no consolidados recientes, con valores de resistividad < 1.372 Ohm.m y profundidades <30 m presenta un buen potencial para el almacenamiento de agua subterránea. Sin embargo, los resultados no son concluyentes sobre el significado hidrogeológico de las estructuras tectónicas para la prospección de aguas subterráneas en el área de estudio.

PALABRAS CLAVE: recursos hídricos subterráneos, tomografía eléctrica de resistividad, lineamentos estructurales, macizo rocoso fracturado, acuífero poroso.

ABSTRACT

The Precambrian metamorphic rocks in the southern region of the Espírito Santo State (southeastern Brazil) is intercepted by ductile and brittle/ductile shear zones over which towns like Guaçuí, Marechal Floriano and Domingos Martins were established. In the years of 2014 to

**Corresponding author: marilane.melo@ufes.br*

1 Departamento de Geologia. Centro de Ciências Naturais e da Saúde, Universidade Federal do Espírito Santo, estado do Espirito Santo, , Brasil

2 Departamento de Geologia Aplicada, Instituto de Geociências e Ciências Exatas, Universidade Estadual Paulista. estado de São Paulo, Brasil

2016 the Espírito Santo State faced the worst drought in the past 80 years. In situations like that, the only source of fresh water available is underground. Therefore, the purpose of this study was to integrate multisource data for groundwater prospecting and management. The study area comprises the central sectors of the Guaçuí and Batatal shear zones. Methodology involved the interpretation of stereo-pairs for the identification of lineaments, electrical resistivity surveys and geological fieldwork. The results were tentatively validated with available groundwater well production data. Six resistivity profiles with a total length of 2,400 m were surveyed and 15 outcrops were described across these structures. Results have shown that the structural framework of the shear zones is predominantly made of NW to NNW and NE to NNE-trending lineaments. The former is related to brittle tectonics and the latter coincides with the ductile Precambrian fabric of the crystalline basement rocks. A near-surface porous aquifer regarded to the regolith and recent unconsolidated sedimentary deposits presenting resistivity values < 1,372 Ohm.m and depths < 30 m have good potential for groundwater storage. However, results are not conclusive about the hydrogeological significance of tectonic structures for groundwater prospection in the study area.

KEY WORDS: groundwater resources, electrical resistivity tomography, structural lineaments, fractured rock mass, porous aquifer.

INTRODUCTION

In rural and urban areas three sources of fresh water resources for human consumption may be available: (a) rivers and water reservoirs; (b) porous aquifers (i.e. soil and sedimentary units); and (c) fractured rock aquifers (Freeze and Cherry, 1979; ANA, 2005). In regions where basement rocks outcrop, groundwater accumulates in opened planar structural features (i.e. joints, faults, foliation, veins, etc.), which serve as a complex conduit-barrier system.

Fractured rock aquifers are controlled by fracture properties such as aperture, spacing (or fracture density), orientation, infillings (e.g. sand, clay, cemented, etc.), roughness (particularly for fractures with small apertures), connectivity, state of stress and nature of host rocks (Costa, 2008; Fernandes, 2008; Singhal and Gupta, 2010; Bense *et al.*, 2013). Fracture network facilitates chemical weathering and dissolution of host rock increasing hydraulic conductivity and groundwater storage (Hiscock, 2005; Brassington 2007).

Unlike fractured aquifers, the literature about the hydrogeological characteristics of rock aquifers related to Precambrian shear zones in Brazil is deficient (Neves and Morales, 2006). Shear zones are tabular regions of concentrated deformation across which adjacent undeformed rock units are offset (Alsop and Holdsworth, 2004). They are linear to curvilinear structures whose length is much greater than width. They are recognized at all scales and can be classified into brittle, ductile and brittle-ductile. Brittle shear zones are characterized by an array of parallel to subparallel fractures and veins, formed under fracturing, brecciation and cataclastic processes in the upper Earth's crust (< 10 km). Ductile shear zones are characterized by the presence of mylonitic rocks, where crystal-plastic deformation processes take place. Typically, such processes occur in the middle to lower Earth's crust. Brittle-ductile shear zones comprise features from both endmembers (Hobbs *et al.*, 1976).

Metamorphic rocks exposed in the southern region of the state of Espírito Santo (Brazil) are cut by the Guaçuí and Batatal NE-trending shear zones (Figure 1). These outstanding structures are tens of kilometers long and can be easily traced from remote sensing and aerogeophysical data (Silva, 2010). From 2014 to 2016 the Espírito Santo state faced the worst drought in the last 80 years according to government agencies, which resulted in water supply problems and economic losses. Some important

locations lay over these features, such as the Guaçuí, Marechal Floriano and the tourist town of Domingos Martins. Population of the three towns combined reach 81,000 inhabitants and land has been extensively used for cattle raising and coffee and eucalyptus plantations (https://cidades.ibge.gov.br/).

In this sense, the aim of this paper is to investigate the hydrogeological significance of these shear zones for groundwater prospecting and management. The use of remote sensing data for the analysis of landforms associated to subsurface geophysical surveys can elucidate the hydrogeological complexity of fractured aquifer system in regions where basement rocks outcrop (Fernandes, 2008; Singhal and Gupta, 2010). Besides, it can assist the conservation of areas of aquifer recharge and the identification of groundwater reservoirs (Dottridgea & Jaber, 1999; Rubin and Hubbard, 2005; Yabel *et al.*, 2015; Salles *et al.*, 2018; Sandoval & Tibujan Jr., 2019). In view of this, we integrate geophysical, remote sensing and geological and structural data.

STUDY AREA

REGIONAL GEOLOGY AND TECTONICS

The Araçuaí orogen, located in southeastern Brazil, and its African counterpart, the West Congo belt, constitute an orogenic system that developed during the Brasiliano-Pan-African orogeny between the margins of the São Francisco and Congo cratons (Alkmim *et al.*, 2006). The Araçuaí-West Congo orogen (A-WC orogen) was formed during the amalgamation of Western Gondwana in Late Neoproterozoic time and split into two parts by the opening of the South Atlantic Ocean in the Cretaceous. The Araçuaí orogen comprises rift-related to distal passive margin sequences, ophiolitic remnants of the precursor Macaúbas basin, Rio Doce magmatic arc-related rocks and pre-collisional to post-collisional intrusions - G1 to G5 Supersuits (Pedrosa-Soares *et al.*, 2011). Paleoproteroic to Archean basement rocks include high-grade metamorphic rocks included in the Caparaó, Juiz de Fora, Ipanema, Guanhães and Serra do Valentim complexes. These represent reworked rocks related to the São Francisco Craton (Vieira *et al.* 2015; Alkmim *et al.* 2006).

The Guaçuí and Batatal NE-trending shear zones are one of the most strikingly geological features encountered in the southern region of the Espírito Santo State and can be easily traced from satellite images and aerogeophysical data for tens to hundreds of kilometers (Figure 1). These geological structures were formed in the final tectonic stages of the A-WC orogen (Pedrosa-Soares *et al.*, 2001; Alkmim *et al.* 2006).

The Guaçuí and Batatal shear zones cross paragneisses belonging to the Paraíba do Sul Complex and pre to late-tectonic granitoids (Vieira, 1997). The Guaçuí Shear Zone (GSZ) is 350 km long and 5 km wide on average and is comprised of mylonites (outer margins) and ultramylonites (core region), showing subvertical mylonitic foliation. The GSZ is a right-lateral ductile shear zone developed under high-grade metamorphism (Cunninghan *et al.*, 1998; Horn, 2007). The Batatal Shear Zone (BSZ) is 70 km long and comprise mylonitic foliation, being interrupted to the south by the post-collisional Iconha pluton (Féboli, 1993; Silva, 2010). According to Silva (2010), the BSZ is a brittle-ductile shear zone originated under low to medium-grade metamorphism.

After a long period of tectonic stability, the Araçuaí-West Congo orogenic belt was broke apart due to the opening of the Atlantic Ocean in the Cretaceous. This tectonic event was responsible for the intrusion of mafic magmatism, uplift of the Serra do Mar mountain range (to the south),

reactivation of inherited geological structures and the development of marginal sedimentary basins, such as the Espírito Santo and Campos basins (Almeida, 1976). The Meso-Cenozoic brittle tectonics in the Brazilian southeastern margin was investigated by many authors (Riccomini, 1995, Ferrari, 2001, Zalán & Oliveira, 2005, Silva & Melo, 2011). In the Espírito Santo State, Ribeiro (2010) and Hartwig and Bozzi (2019) recognized three brittle deformation phases responsible for landform development and deformation of the semi-consolidated sediments of the Barreiras Formation (Miocene). Calegari *et al.*, (2016) recognized a NW-trending Lineament in the Espírito Santo southeastern margin, named as the Alegre Fracture Zone, originated in the Cambrian Period and reactivated in the Cenozoic Era. Lourenço *et al.* (2016) obtained similar results for the Piúma lineament, a 70 km long and N50W-trending brittle shear zone. Maizatto *et al.* (2009) apud Chemale Jr & Hadler (2005) based on apatite fission tracks analysis, recognized an important tectonic event during 80-60 Ma in the south-central Espírito Santo State, which caused a regional uplift that reached up to 3,000 m.

Few stress data are available for the southern Brazil (Lima *et al.*, 1997). According to the authors, measurements obtained from breakout for 145 wells in the Campos, Santos and Espírito Santo offshore basins are too scattered to define a regional SH_{max} orientation.

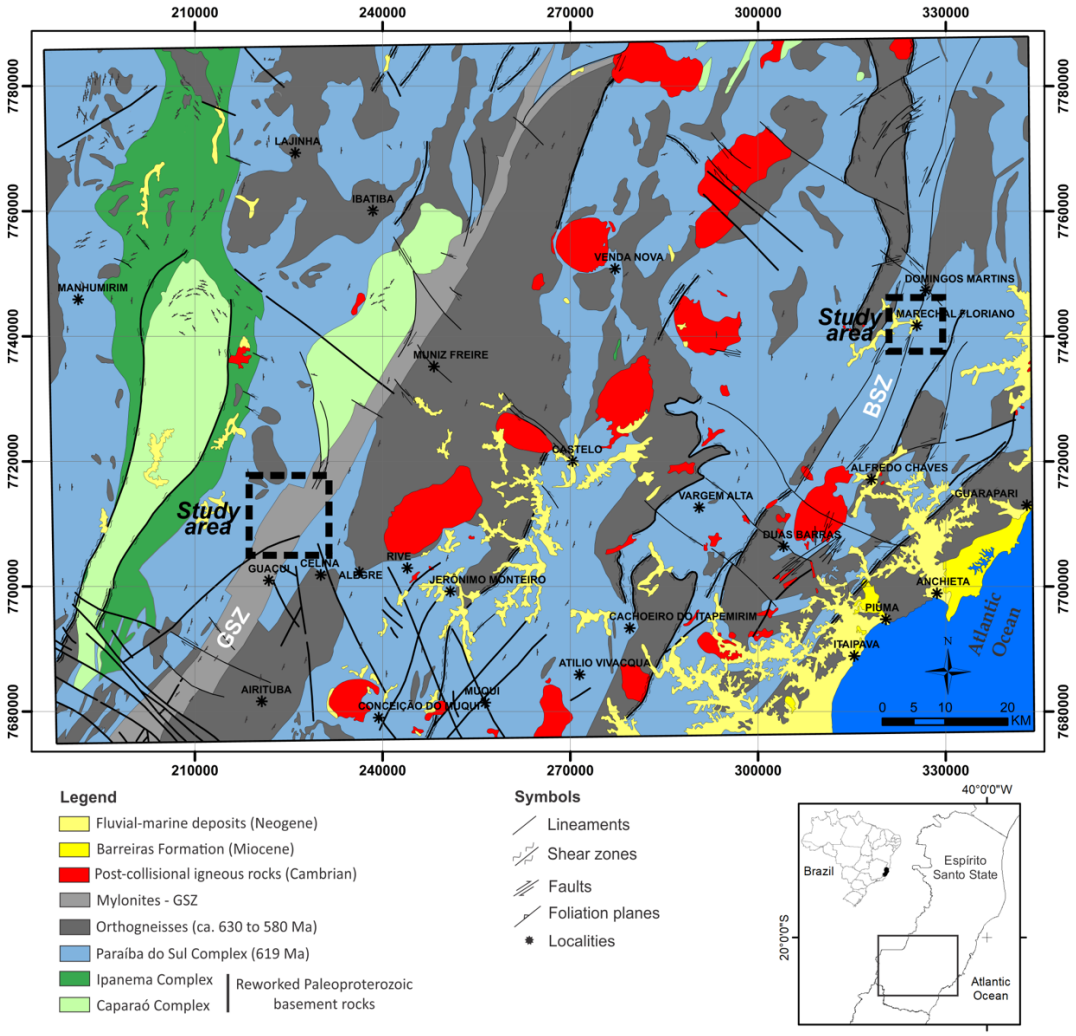

Figure 1. Regional geology of the study area based on Vieira (1997).

Soils and Landforms

Landforms in the study area are included in the Mantiqueira Northern Plateau geomorphological unit (Gatto *et al.* 1983). They are structurally controlled by NE to NNE-trending lineaments inherited from basement rocks as well as NW-trending lineaments. Hilly landforms with rounded summits and gentle to steep slopes predominate. Landscape is marked by a regional plateau around 700 m.a.s.l amid which rocky domes emerge, reaching elevations up to 1,700 m.a.s.l. These are usually associated to post-collisional igneous rocks.

Alluvium deposits are associate to the drainage system. They are made of a mixture of gravel, sand and clay (Vieira, 1997). Soil profile can reach tens of meters in regions where elevations are moderate to gentle and gneissic rocks occur. Soil is described as red and yellow latosols, podzols and cambisols (Panoso *et al.* 1978). Colluvium soils and talus are observed close to rock domes, which are very common in landscape.

Climate and Surface Hydrology

According to Köppen climate classification, Guaçuí town has an Aw (tropical savanna) climate type and Domingos Martins town has a Cfa (humid subtropical) climate type (https://pt.climate-data.org/). Guaçuí and Domingos Martins towns have average annual temperature around 21 degrees Celsius and average precipitation around 1,200 mm/year, with rainfalls occurring preferentially between October and March. The driest month occur in June and the rainiest month occur in December.

Drainage network is structurally controlled (Vieira, 1997). Itabapoana and Jucu rivers are the regional base level in the Guaçuí and Domingos Martins areas, respectively. Domingos Martins municipality has currently two small hydroelectric power stations in operation (< 30 MW) in the Jucu river and Guaçuí municipality has one (55 MW) in the Itabapoana river (www.annel.gov.br). River levels oscillate few meters along the year as a function of rainfall and seasons.

Materials and Methods

The methodology of this work involved the integration of remote sensing, structural and electrical resistivity data (Madrucci *et al.*, 2005; Fernandes, 2008; Francese *et al.* 2009). Cartographic data were georreferenced in ArcGIS 10.4 (ESRI, 2015) using the horizontal Datum WGS-84 and the UTM map projection (Zone 24S). All data surveyed in this work was overlapped and integrated in the ArcGIS software.

The first step consisted in the interpretation of aerial photographs of the extinct Brazilian Coffee Institute – IBC (scale 1:30,000) freely available for the state of the Espírito Santo at the GEOBASES portal (https://geobases.es.gov.br/imagens-es-ibc-gerca-1970). The ST4 WILD Heerbruggg stereoscope was used for photogeological analysis. 11 stereo-pairs were studied and integrated for the GSZ and 5 stereo-pairs were used for the BSZ. Photogeological interpretation followed the procedures described in Soares and Fiori (1976) and Arcanjo (2011). The focus of the photogeological analysis was the identification of lineaments, which represent favorable features for groundwater storage. The term lineament used in this work followed the definition presented by O'Leary *et al.*, (1976). Aerial photos were georeferenced based on the Divino de São Lourenço and Domingos Martins topographic maps – scale 1:50,000 (IBGE, 1977 and 1978) and satellite images from GoogleEarth.

Fieldwork included the description and classification of lithologies (Fettes & Desmons, 2014) and description and collection of structural data (McClay, 1991). Structural data orientation was interpreted based on Schmidt-Lambert stereograms (Hobbs *et al.* 1976). For the study of the GSZ, eight outcrops distributed in 16 km were described along the roads ES-185 and ES-387, between the district of Celina and the small town of Ibitirama (Figure 1). For the study of the BSZ, 7 outcrops distributed in 9.7 km were described along the road BR-262.

The electrical resistivity method has been largely used for the survey of groundwater in fractured aquifers (Gallas, 2003; Braga, 2016; Singh *et al.* 2019; Briški *et al.* 2020). Usually, fractures represent permeable zones filled with water and/or soil/chemically weathered rock. Thus, they tend to present lower values of resistivity in comparison with adjacent intact rock mass. The electrical resistivity prospecting consisted in the use of the DC Resistivity method through the electrical resistivity tomography technique in a Schlumberger electrode array, distributed along six profiles with 10 meters of electrode spacing. Six resistivity profiles with a total length of 2,480 m were surveyed. A total of 385 measurements were determined for the profiles 380 m long and 527 measurements for only one profile 580 m long. The maximum investigation depth reached up to 130 m. Geophysical survey lines were preferentially setted up in the outer margins and inner portions of the GSZ and BSZ. They are oriented parallel and perpendicular to these structures.

The geophysical equipment used was the Terrameter LS resistivity meter, manufactured by ABEM Instrument (Sweden), which consists of a single automated signal transmission and reception module, with 250 W of power, 1 μV resolution and maximum electric current of 2.5 A (ABEM 2012).

Data acquired in the field were processed in the RES2DINV computational program (Geotomo, 2003). The results comprise resistivity profiles of distance versus depth presented in logarithmic scale in which values are interpolated and displayed in intervals of colors. This program automatically determines a two-dimensional subsurface model, from resistivity or chargeability data obtained in electrical profiling tests (Griffiths & Barker 1993).

The 2D model used in the program divides the pseudo-section into rectangular blocks, which will represent the pseudo-section by adjusting the field measurements. This optimization aims to reduce the difference between the apparent resistivity values calculated and measured in the field by adjusting the resistivity of the block model. The difference between the values is expressed by the root mean squared error (RMS) and its product is represented as inversion models (Loke & Barker 1996).

In order to validate the results, an attempt was made by comparing geoelectric profiles with groundwater well production data freely available in the CPRM-SIAGAS portal at http://siagasweb.cprm.gov.br/layout/visualizar_mapa.php.

RESULTS

PHOTOGEOLOGICAL ANALYSIS OF AERIAL STEREO-PAIRS

Structural lineaments interpreted from aerial stereo-pairs for the GSZ are displayed in Figure 2. 1,148 lineaments were interpreted and are distributed in 120 km^2. Lengths varied from 52 m to 3,866 m; average value equals to 386 m. NW and NE-trending lineaments predominate, respectively. NE-trending lineaments are concentrated in the eastern and southern portions of

the study area (Figure 2), which coincides with the main trace of the GSZ. The NW portion of Figure 2 shows a distinct structural pattern in terms of orientation and lineament density (aerial photos ES-23 - 4505 and ES-23 - 4506).

Structural lineaments interpreted from aerial stereo-pairs for the BSZ are displayed in Figure 3. 490 lineaments were interpreted and are distributed in 78 km^2. Lengths varied from 79 to 4,155 m;average value equals to 418 m. NW-trending lineaments predominate but are scattered between N295 to N335. Structural domains are not evident.

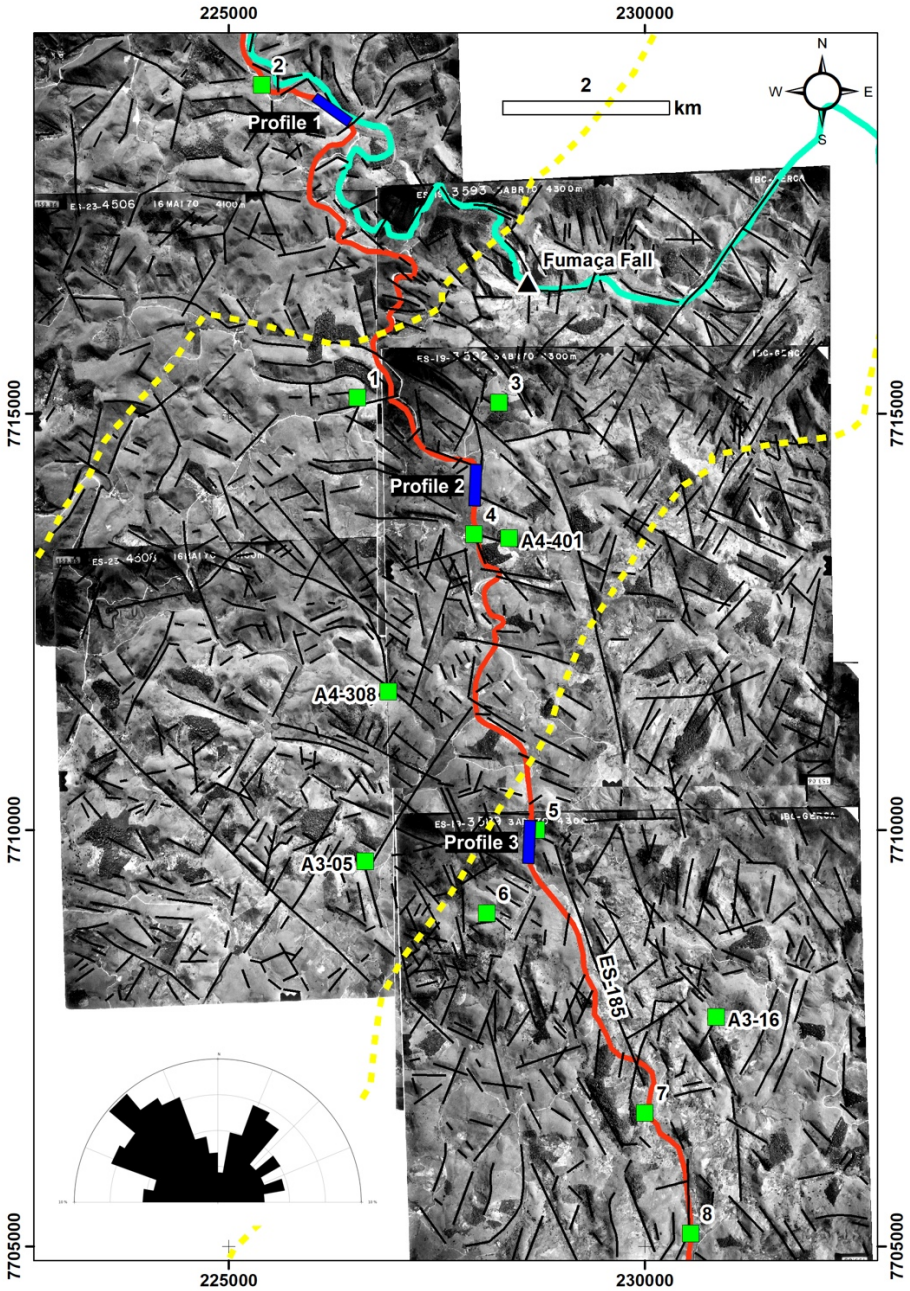

Figure 2. Structural map interpreted from aerial stereo-pairs for the BSZ with indication of the studied outcrops (labeled green boxes) and resistivity profiles (labeled blue rectangles). In the lower left corner, rose diagram display lineament orientations. Red line – roads and yellow dashed line – GSZ (after Horn, 2007).

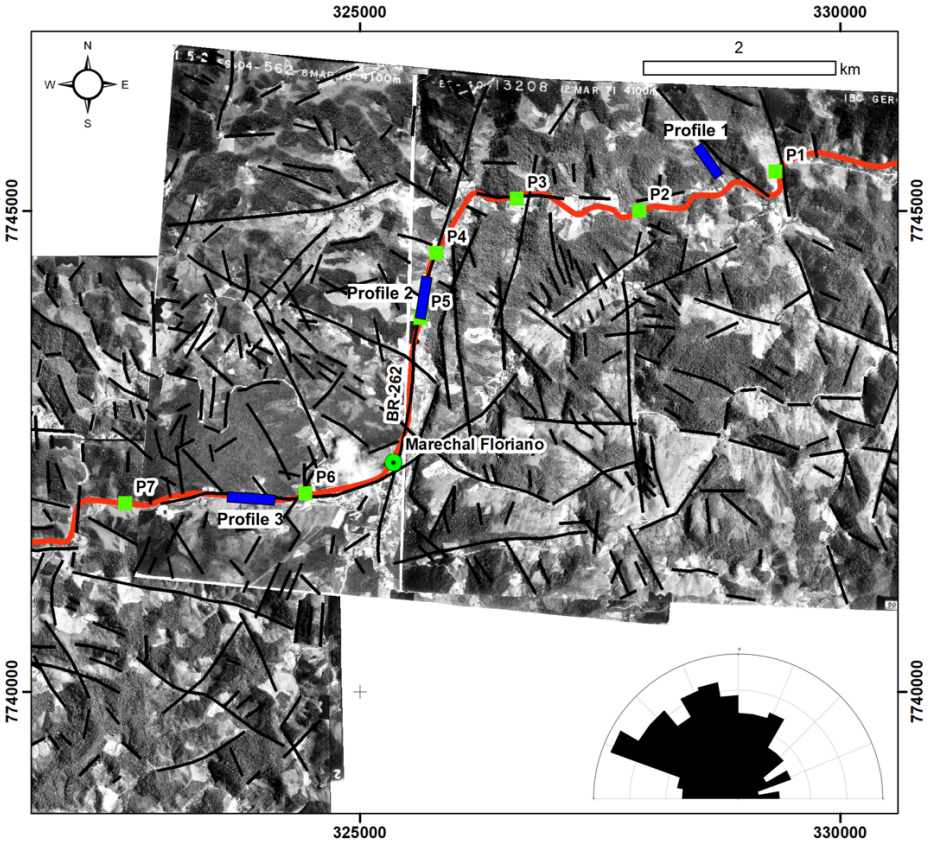

Figure 3. Structural map interpreted from aerial stereo-pairs for the BSZ with indication of the studied outcrops (labeled green boxes) and resistivity profiles (labeled blue rectangles). In the lower right corner, rose diagram display lineament orientations. Red line – road BR-262. According to Féboli (1993), the BSZ follow the Batatal river and passes through P4 and P5 rock outcrops.

FIELD GEOLOGICAL AND STRUCTURAL DATA

Fieldwork reveled three main lithotypes for the Guaçuí Shear Zone. In outcrop 8 occurs metagranites and in outcrops 1, 2 and 7, orthogneisses (Figure 2). In all the other outcrops are exposed mylonitic rocks (3, 4, 5, 6, A03-05, A03-16, A04-308 and A04-401). Besides, in one outcrop very close to Point 4 (UTM 24S 227154E/7713215S) a stromatic metatexite was also described. It shows a subvertical and penetrative foliation oriented parallel to the GSZ. Metagranites are coarse-grained and leucocratic rocks with weak foliation defined by mm-sized biotite crystals. Orthogneisses are course to fine-grained rocks and show remarkable cm-sized gneissic banding. Deformed mafic enclaves, few decimeters in size, and sparingly migmatized zones are also observed. Mylonitic rocks show typical cm to mm-sized mylonitic banding and numerous dextral kinematic indicators.

Figure 4 depicts stereograms of the planes of foliation along the cross-section studied. The results indicate that predominates strikes ranging from NNW to NNE and moderate to steep dip angles (45 - 64°) dipping predominantly to the east. Field observations across the GSZ revealed slightly fractured rock masses.

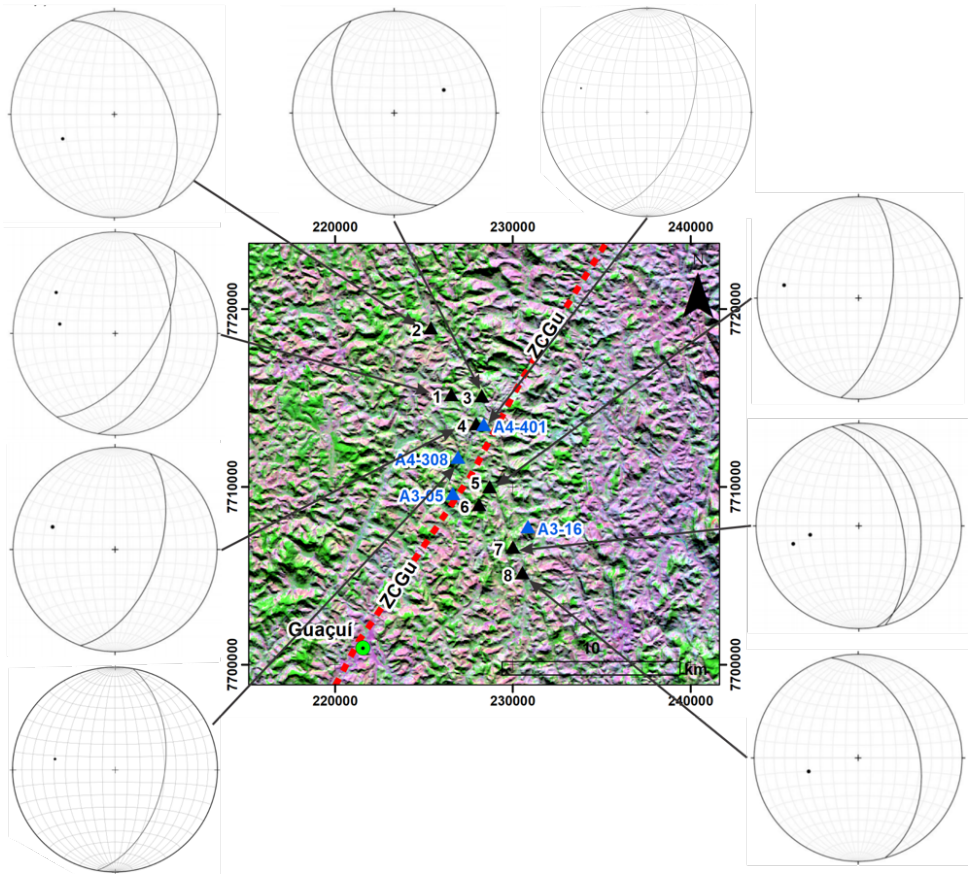

Figure 4. Stereographic projection of the planes of foliation across GSZ. Schmidt-Lambert net, lower hemisphere (equal area). Black triangles studied outcrops (this study) and blue triangles (Hartwig & Melo, 2019). Background image: Landsat-5 5R4G3B colored composition.

The transect course across the BSZ revealed coarse-grained garnet biotite gneiss, garnet metagranodiorite to metatonalite and calcisilicatic rocks. Gneissic banding is made of alternating and parallel mafic and felsic banding. Banding thickness ranges from 0.1 to 3.0 cm in hand specimens. Mafic bands are essentially made of biotite and garnet crystals and felsic bands are made of quartz, K-feldspar and plagioclase grains. A fine-grained banded calcisilicatic rock was identified in outcrop 3. Deformed mafic enclaves and sinistral kinematic indicators were observed in outcrop 6. A course-grained sillimanite-garnet gneiss was described in outcrop 7. Garnet metagranodiorites to metatonalites were recognized in outcrops 1, 2 and 5 and show a metamorphic foliation characterized by undulose films of biotite flakes (< 1 mm in diameter on average).

Figure 5 depicts stereograms of foliation along the cross-section studied. NE to NNE-trending foliation with dip angles ranging from 10 to 88° predominates. In outcrops 1, 2 and 3, a NW-trending foliation is observed with dip angles ranging from 20 to 60°. Outcrops described across the BSZ revealed slightly fractured rock masses.

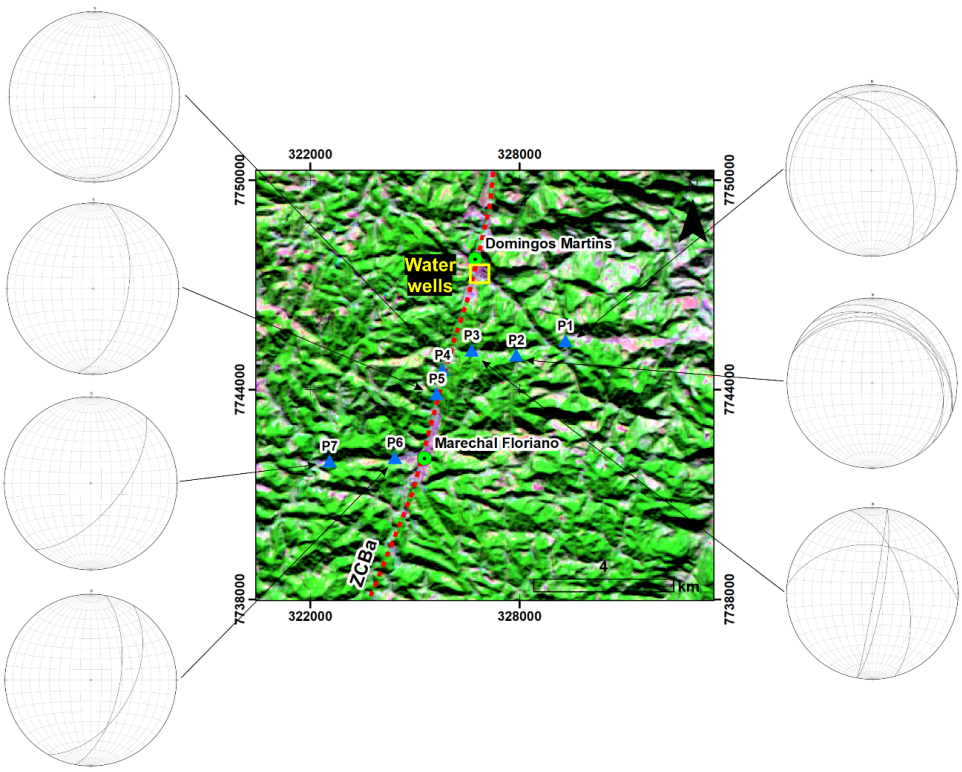

Figure 5. Stereographic projection of the planes of foliation across BSZ. Schmidt-Lambert net, lower hemisphere (equal area). Blue triangles, studied outcrops. Small yellow rectangle indicates the area where groundwater wells are distributed. Background image: Landsat-5 5R4G3B colored composition.

ELECTRICAL RESISTIVITY TOMOGRAPHY

Geophysical investigation depths ranged from 80 to 130 m for the Guaçuí Shear Zone (Figure 6). Resistivity profiles 1 and 3 are located in the west and east outer margins of the GSZ and resistivity Profile 2 is located within it (Figure 2). Resistivity profiles allow interpreting two geoelectrical layers. A superficial one regarded as soil/recent sedimentary deposits (containing groundwater or not) and a competent, unfractured and fresh rock mass (sound rock).

Resistivity profiles 1 and 2 show increasing values of electrical resistivity with depth ranging from approximately 117 to 16,070 Ohm.m. Resistivity profiles 1 and 2 show a saturated and discontinuous horizontal aquifer between elevations 710 and 660 m.a.s.l, exhibiting very low electrical resistivity values (< 117 Ohm.m). Resistivity Profile 3 shows a horizontal layer of very high electrical resistivity values (> 16,070 Ohm.m) between elevations 675 and 645 m.a.s.l, surrounded by moderate values of resistivity (~ 1,372 Ohm.m). The distribution pattern of the electrical resistivity isovalues under this layer may indicate the presence of a subhorizontal fracture. Lineaments interpreted from stereo-pairs are not evident in the resistivity sections of Figure 6 as disturbances in the distribution and magnitude of resistivity values are not discernable.

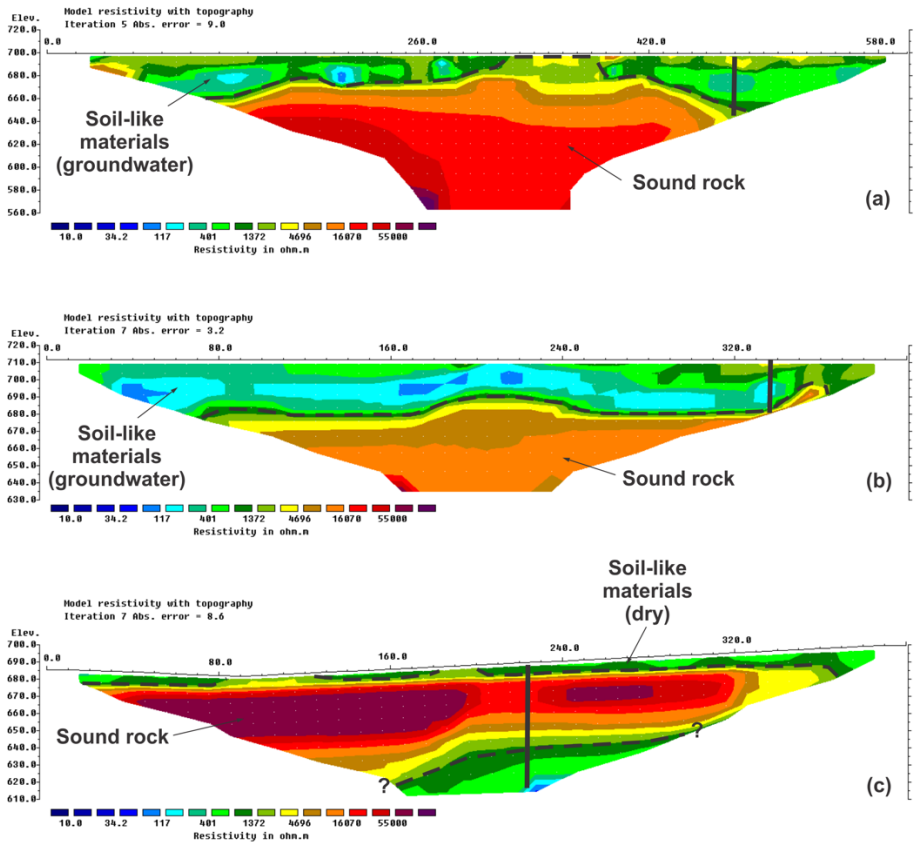

Figure 6. 2D eletrical resistivity imaging pseudosections for the GSZ in Ohm.m: (a) Resistivity Profile 1; (b) Resistivity Profile 2; and (c) Resistivity Profile 3. Dashed lines refer to geological contacts and fractures interpreted directly from resistivity sections, while continuous lines refer to lineaments based on the interpretation of stereo-pairs.

Geophysical investigation depths for the Batatal Shear Zone ranged from 75 to 85 m (Figure 7). Resistivity profiles are oriented parallel and perpendicularly to the main structural trends. Resistivity profiles 1 and 3 are located in the east and west outer margins of the BSZ while resistivity Profile 2 is within it (Figure 3). Resistivity Profile 1 shows in general average values of electrical resistivity (~ 1,372 Ohm.m) that indicate highly weathered rock masses (saprolite). Between electrodes located from 160 to 210 m, a huge elliptical spot of very high electrical resistivity is observed (55,000 Ohm.m) from elevations 515 to 485 m.a.s.l. Very high values of electrical resistivity indicate sound rock. Resistivity Profile 1 also indicates an irregular shaped layer (probably dry soil) dipping gently to the left.

Resistivity Profile 2 shows two regions of low values of electrical resistivity that indicate saturated soil/recent sedimentary deposits, separated by a central portion of high electrical resistivity values (> 4,696 Ohm.m). The vertical lineament interpreted from the stereo-pairs in the central portion of the section does not produce significant changes in the distribution pattern of resistivity isovalues.

Resistivity Profile 3 shows a superficial horizon of saprolite (1,372 Ohm.m) underlaid by sound rock (4,696 Ohm.m). Two spots of very high electrical resistivity values are observed (> 16,070 Ohm.m) between electrodes located at 180-210 m and 300-370 m. The central portion of resistivity Profile 3 also exhibits a distribution pattern of electrical resistivity values that suggests the presence of subvertical geological structures.

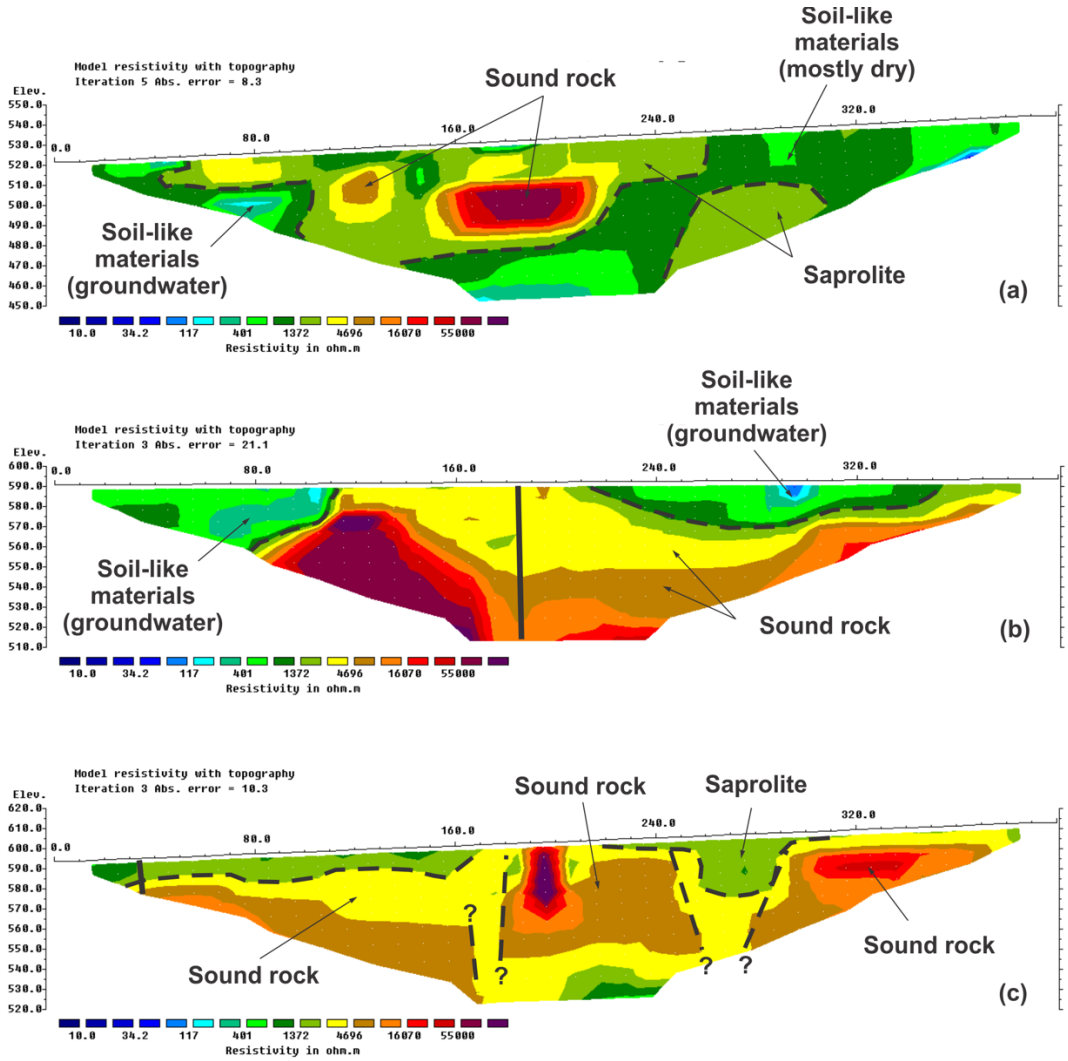

Figure 7. 2D eletrical resistivity imaging pseudosections for the BSZ in Ohm.m: (a) Resistivity Profile 1; (b) Resistivity Profile 2; and (c) Resistivity Profile 3. Dashed lines refer to geological contacts and fractures interpreted directly from resistivity sections, while continuous lines refer to lineaments based on the interpretation of stereo-pairs.

DISCUSSIONS

The geological interpretation of remote sensed data revealed that NW and NE-trending lineaments are the most important structures. NE-trending lineaments coincides with the orientation of ductile structures of the Precambrian crystalline basement rocks. NW-trending structures are associated to the opening and evolution of the South Atlantic Ocean (Calegrari *et al.*, 2016; Lourenço *et al.*, 2016). Hartwig and Bozzi (2019) recognized more than one hundred NW and NE-trending fractures in the semi-consolidate Miocene sediments of the Barreiras Formation in the southern margin of the Espírito Santo State showing that both sets were reactivated in recent times. For BSZ, the lineaments orientations are more scattered in comparison with the GSZ (Figures 2 and 3). Remote sensed data have also shown that the GSZ (9.5 lineaments/km^2) is more structured than the BSZ, (6.3 lineaments/km^2). Moreover, the GSZ is more strongly controlled by NE-trending lineaments.

Geological and structural field data revealed poorly fractured rock masses. Some fractures identified in the field are related to rock blasting and does not have hydrogeological significance. Foliations are predominantly oriented from NNW to NE for both shear zones. The GSZ shows a penetrative milonitic foliation while for the BSZ rocks show a weak metamorphic foliation with significant variations in dip angles.

Geophysical surveys clearly revealed a superficial porous aquifer in both shear zones, which is associated to low values of resistivity. Although the GSZ present numerous geological lineaments when viewed from stereo-pairs, resistivity sections have not confirmed their subsurface expression. One possible explanation for that may be due to their limited lengths. The low values of resistivity that appear bellow elevation 640 m.a.s.l. in Figure 6c seems to be related to exfoliation joints. These are widely regarded as forming in response to removal of overburden, associated to landform evolution (Hartwig, 2006; Hobbs *et al.* 1976, Bahat *et al.* 1999).

Abrupt changes in the orientation of the resistivity isolines indicate a fractured rock mass for the BSZ (Figure 7c). However, these structures seem to be related to sealed (closed) fractures as high resistivity values (> 4,696 Ohm.m) predominate elsewhere. Telford *et al.* (1990) present examples of electrical resistivity values for common rocks and minerals. Considering geological fieldwork data, it is possible to interpret that the distribution and magnitude patterns of resistivity values observed in Figure 7c may be related to faciological differences in crystalline basement rocks.

According to Costa (2008) and Fernandes (2008) not only the degree of fracturing, but also the principal horizontal stress orientation control groundwater storage and flow in fractured aquifers. Ribeiro (2010) studied the brittle tectonics of the Barreiras Formation in the southern margin of the Espírito Santo state and recognized NW-oriented sinistral strike-slip faults. According to the author, they were originated by extensional stress-oriented NE-SW, associated to a Quaternary E-W-trending dextral strike-slip tectonic regime. Therefore, if this state of stress was still active, groundwater would be more likely retained in NW-trending lineaments.

Groundwater production data from tube wells is available only for the BSZ (Table 1). Ten groundwater wells are distributed in Domingos Martins urban area (Figure 5). Well production data is available for only five of them. Flow rates for these water wells ranged from 0.4 to 19.8 m^3/h. It is worth mentioning that all groundwater wells lay over a long NW-trending lineament (Figure 5). However, information regarding the geology crossed by these wells and filter positions was not provided.

Figure 8 summarizes rock mass conceptual models for groundwater prospection for both the GSZ and the BSZ. A potential superficial porous aquifer is regarded to unconsolidated sedimentary deposits and/or soil cover (regolith). This are concentrated in the first 30 meters below surface and is well developed in the GSZ (Figures 6a,b). Although it is easily exploited for human consumption, it is also very vulnerable to pollution, especially from wastewater (Bertossi *et al.* 2013). Poorly fractured rock masses are associated to the GSZ and fractured rock masses were recognized for the BSZ (Figure 7c). Nevertheless, discontinuities seem to be sealed (closed) as high resistivity values (> 4,696 Ohm.m) predominate elsewhere.

Table 1. Well production data for the BSZ. Source: CPRM-SIAGAS.

Well codes	Locality	E (m)	N (m)	Flow rate (m^3/h)
3100016741	Campinho- Domingo Martins	326,741.2	7,747,191.8	19.8
3100016744	Campinho-Domingos Martins	326,971.61	7,747,347.9	0.4
3100016745	Campinho-Domingos Martins	326,970.99	7,747,409.45	6
3100016746	Campinho- Domingos Martins	327,03028	7,747,287.05	2.8
3100016747	Campinho-Domingos Martins	327,001.87	7,747,225.2	3

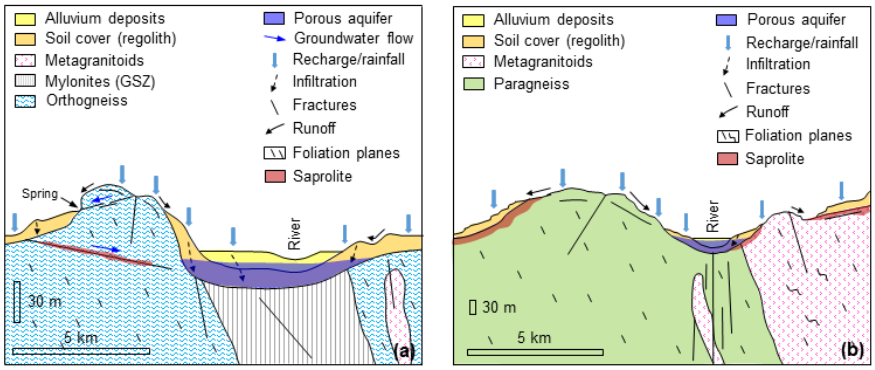

Figure 8. Rock mass conceptual model for groundwater prospection for the GSZ (a) and the BSZ (b).

CONCLUSIONS

The aim of this paper was to investigate the hydrogeological significance for groundwater prospecting of two Precambrian NE-trending shear zones, located in the southern region of the Espírito Santo State (Southeastern Brazil).

Based on the results, a porous near-surface aquifer has good potential for groundwater storage, especially in the GSZ. The GSZ and the BSZ are intercepted by numerous lineaments preferentially oriented to NE-NNE and NW-NNW. The former is associated to ductile Precambrian tectonics (Araçuaí-West Congo Orogen) while the latter to Meso-Cenozoic brittle tectonics. However, integrated data is not conclusive about the hydrogeological significance of brittle and ductile discontinuities for groundwater prospection. The resistivity profiles and available water well data did not confirm the occurrence of groundwater associated with them, which may be due to the amount of surveyed data, state of stress, etc. Authors recommend more investigations in the north and south sectors of the GSZ and the BSZ in order to better understand the hydrogeological significance of these geological features.

REFERENCES:

ABEM, 2012, Terrameter LS - Instruction Manual. ABEM Instrument AB: Sundbyberg, 1-122.

Almeida F.F.M.de., 1976, The System of Continental Rifts bordering the Santos Basin, Brazil. *An. Acad. Bras. Ciênc.*, 48, 15-26.

ANA – Agência Nacional das Águas. Disponibilidade e demandas de recursos hídricos no Brasil. Available on: < http://arquivos.ana.gov.br/planejamento/planos/pnrh/VF%20DisponibilidadeDemanda.pdf> Access on: November 10, 2019.

Alkmim F.F., Marshak S., Pedrosa-Soares A.C., Peres G.G., Cruz S.C.P., Whittington A., 2006, Kinematic evolution of the Araçuaí-West Congo Orogen in Brazil and Africa: nutcracker tectonics during the Neoproterozoic assembly of Gondwana. *Precambrian Research*, 149, 43-64.

Arcanjo J. B. A., 2011, Fotogeologia: conceitos, métodos e aplicações. CPRM/SGB, Salvador. Brasil, 144.

Alsop G.I., Holdsworth R.E., 2004, Shear zones — an introduction and overview. Geological Society, London, Special Publications, 224, 1-9. https://doi.org/10.1144/GSL.SP.2004.224.01.01.

Bahat D., Grossenbacher K., Karasaki K., 1999, Mechanism of exfoliation joint formation in granitic rocks, Yosemite National Park. *Journal of Structural Geology*, 21, 85-96.

Bense, V.F., Gleeson T., Loveless S.E., Bour, O., Scibek, J., 2013, Fault zone hydrogeology. *Earth-Science Reviews*. v. 127. p. 171-192.

Bertossi, A. P. A., Cecílio, R.A., Neves, M.A., Garcia, G,O. 2013. Qualidade da água em microbacias hidrográficas com diferentes coberturas do solo no sul do Espírito Santo. *Rev. Árvore*, v. 37, n. 1, p. 107-117.

https://doi.org/10.1590/S0100-67622013000100012.

Braga, C.O. Geofísica Aplicada: Métodos Geoelétricos em Hidrogeologia. São Paulo: Editora Oficina de Textos. 2016, 159.

Brassington R., 2007, Field Hydrogeology. Chichester, Jonh Wiley & Sons, 312.

Briški M., Stroj A., Kosović I., Borović S., Characterization of aquifers in metamorphic rocks by combined use of electrical resistivity tomography and monitoring of spring hydrodynamics. *Geosciences*, 10, 137, 2-18. doi:10.3390/geosciences10040137.

Calegari S.S., Neves M.A., Guadagnin F., França G.S., Vincentelli M.G.C., 2016, The Alegre Lineament and its role over the tectonic evolution of the Campos Basin and adjacent continental margin, southeastern Brazil. *Journal of South American Earth Sciences*, 69, 226-242.

Costa W.D., 2008, Hidrogeologia dos meios fraturados. In: Feitosa, A.C., Filho, J.M., Feitosa, E.C., Demetrio, J.G.A. *Hidrogeologia: conceitos e aplicações.* 3ª Ed. Rio de Janeiro: CPRM/LABHID, 121-151.

Cunningham, D.; Alkmim, F.F.; Marsakh, S., 1998, A structural transect across the coastal mobile belt in the Brazilian Highlands (latitude 20°S): the roots of a Precambrian transpressional orogen. *Precambrian Research*, 92, 251-275.

Dottridgea J., JABER N.A., 1999, Groundwater resources and quality in northeastern Jordan: safe yield and sustainability. *Applied Geography*, 19, 4, 313-323. https://doi.org/10.1016/S0143-6228(99)00012-0.

Gatto L.C.S.; Ramos V.L.S.; Nunes B.T.A.; MamedE L.; Góes M.H.B.; Mauro C.A.; Alvarenga S. M.; Franco E. M. S.; Quirico A. F.; Neves L. B. Geomorfologia. In: Projeto RADAMBRASIL, Folhas SF.23/24 Rio de Janeiro/Vitória; geologia, geomorfologia, pedologia, vegetação e uso potencial da terra, Rio de Janeiro, IBGE. 1983, 305-384.

ESRI 2015. ArcGIS Desktop: Release 10.4. Redlands, CA: Environmental Systems 498 Research Institute.

Fernandes A.J., 2008, Aquíferos fraturados: uma revisão dos condicionantes geológicos e dos métodos de investigação. *Revista do Instituto Geológico*, 29, 1/2, 49-72.

Féboli W.L. (Org.)., 1993, Programa de Levantamentos Geológicos Básicos do Brasil. Texto Explicativo e Carta Geológica – escala 1:100.000, Folha Domingos Martins-ES – SF.24-V-A-III. DNPM/CPRM., 179.

Ferrari A.L., 2001, Evolução tectônica do Gráben da Guanabara. PhD thesis. Universidade de São Paulo. São Paulo, 412.

Fettes D., Desmons J., 2014, Rochas metamórficas: classificação e glossário. Tradução de: Neto, J.M.R. São Paulo: Oficina de Textos, 313.

Francese R., Mazzarini F., Bistacchi A., Morelli G., Pasquarè G., Praticelli N., Robain H., Wardell N., Zaja A., 2099, A structural and geophysical approach to the study of fractured aquifers in the Scansano-Magliano in Toscana Ridge, southern Tuscany, Italy. *Hydrogeology Journal*, 17, 1233-1246.

Freeze R.A., Cherry J.A., 1979, Groundwater. New Jersey, U.S.A: Prentice-Hall, 604.

Gallas J.D.F., 2003, Prospecção de água subterrânea em aquíferos cristalinos com o emprego de métodos indiretos. *Revista do Instituto Geológico*, 24, 1/2, 43–51.

GEOTOMO SOFTWARE, 2003, RES2DINV (v.3.54) for 98/ME/2000/NT/XP. Geoelectrical Imaging 2D and 3D.

Griffiths D.H., Barker, R.D., 1993, Two-dimensional resistivity imaging and modelling in areas of complex geology. *Journal of Applied Geophysics*, 29, 211-226. https://doi.org/10.1016/0926-9851(93)90005-J.

Hartwig M.E., Bozzi A.H.R., 2019, Análise neotectônica da Formação Barreiras na porção sudeste do estado do Espírito Santo. In: XVII Simpósio Nacional de Estudos Tectônicos. *Anais*… Bento Gonçalves, Brasil, SBG, 26, 29, 148.

Hartwig M. E., Melo M. G., 2019, Sobre o Lineamento Guaçuí em seu segmento central: aspectos metamórficos e microestruturais. In: XVII Simpósio Nacional de Estudos Tectônicos. *Anais*… Bento Gonçalves, Brasil, SBG, 26, 29, 15.

Hartwig M.E., 2006, Tectônica rúptil mesozoica-cenozoica na região da Serra dos Órgãos, RJ. Master thesis. Universidade de São Paulo, São Paulo, 117.

Hiscock K.M., 2005, Hydrogeology: principles and practice. Oxford, Blackwell Publishing, 405.

Hobbs B.E., Means W.D., Williams P.F., 1976, An outline of structural geology. Wiley, New York, 571

Horn A.H, 2007, Programa Geologia do Brasil. Levantamentos Geológicos Básicos. Geologia da Folha Espera Feliz. Follha SF.24-V-A-IV. Escala 1:100.000. Brasília: CPRM., Brasil.

Instituto Brasileiro de Geografia e Estatística – IBGE, 1977, Folha Topográfica Divino de São Lourenço - Folha SF-24-V-A-IV-2. Escala 1:50.000, Brasil.

Instituto Brasileiro de Geografia e Estatística – IBGE, 1978. Folha Topográfica Domingos Martins - Folha SF-24-V-A-III-4. Escala 1:50.000., Brasil.

Lima C., Nascimento E., Assumpção, M., 1997, Stress orientations in Brazilian sedimentary basins from breakout analysis: implications for force models in the South American plate. *Geophys. J. Int*, 130, 112-124.

Loke M.H., Barker R.D, 1996, Rapid least-squares inversion of apparent resistivity pseudosections by a quasi-Newton method. *Geophysical Prospecting*, 44, 131-152. doi: 10.1111/j.1365-2478.1996.tb00142.x

Lourenço F.S., Alkmim F.F., Araújo M.N.C., Romeiro M.A.T., Matos G.C., Crósta, A.P, 2016, The Piúma Lineament, southern Espírito Santo: structural expression and tectonic significance. *Brazilian Journal of Geology*, 46, 4, 531-546.

Madrucci V., Taioli F., Araújo C.C.D., 2005, Análise integrada de dados de sensoriamento remoto, geologia e geofísica no estudo de aqüífero fraturado, Lindóia-SP. *Revista Brasileira de Geofísica*, 23, 4, 437–451.

Maizatto J.R., Lana C.C., Ribeiro A.W.S., Ferreira E.P, 2008, Evidências de terras altas no Campaniano da bacia do Espírito Santo. *Boletim Geociências Petrobrás*, 17, 1, 31-43.

Mcclay K. R., 1991, The mapping of geological structures. Chichester: Wiley, 161.

Medeiros Júnior, E. B. 2016. Evolução petrogenética de terrenos granulíticos nos estados de Minas Gerais e Espírito Santo. Tese de Doutorado, Escola de Minas, Universidade Federal de Ouro Preto, Ouro Preto.

Neves M. A., Morales, N, 2006, Well productivity-controlling factors in crystalline terrains of Southeastern Brazil. *Hydrogeology Journal*, 15, 471-482.

O'leary D. W., Friedman J. D., Pohn, H. A, 1976, Lineament, linear, lineation: some proposed new standards for old terms. *Geological Society American Bulletin*, 87, 1463 – 1469.

Panoso L.A., Gomes L.A., Pires Filho A.M., Bonelli S, 1978, Levantamento de reconhecimento de solos do Estado do Espírito Santo. Rio de Janeiro: EMBRAPA-SNLCS., 461 (Boletim Técnico Nº 45)

Pedrosa-Soares A.C., De Campos C.P., Noce C., Silva L.C., Novo T., Roncato J., Medeiros S., Castañeda C., Queiroga G., Dantas E., Dussin I., Alkmim F, 2011, Late Neoproterozoic–Cambrian granitic magmatism in the

Araçuaí orogen (Brazil), the Eastern Brazilian Pegmatite Province and related mineral resources. Geological Society of London, Special Publication., 350, 25–51.

Pedrosa-Soares A.C., Noce C.M., Wiedemann C., Pinto C.P, 2001, The Araçuaí-West Congo Orogen in Brazil: an overview of a confined orogen formed during Gondwanaland assembly. *Precambrian Research*. 110, 307–323.

Ribeiro C. S, 2010, Influência da tectônica pós-deposicional na distribuição da Formação Barreiras entre o rio Paraíba do Sul (RJ) e o rio Doce (ES). Master thesis. Universidade Federal do Rio de Janeiro – UFRJ, 165.

Riccomini C, 2005, Padrão de fraturamento do maciço alcalino de Cananéia, estado de São Paulo: relações com a tectônica mesozóico-cenozóica do sudeste do Brasil. Revista Brasileira de Geociências. 1995, 25, 2, 79-84.

Rubin Y.; Hubbard S.S. Hydrogeophysics. Dordrecht, Springer, 527.

Salles L.A., Lima J.E.F.W, Roig H.L., Malaquias, V, 2018, Environmental factors and groundwater behavior in an agricultural experimental basin of the Brazilian central plateau. *Applied Geography*, 94, 272-281. doi: 10.1016/j.apgeog.2018.02.007

Sandoval J.A., Tiburan JR. C.L, 2019, Identification of potential artificial groundwater recharge sites in Mount Makiling Forest Reserve, Philippines using GIS and Analytical Hierarchy Process. *Applied Geography*, 105, 73-85. doi: 10.1016/j.apgeog.2019.01.010.

Silva C. M. T., 2010, O sistema transcorrente da porção sudeste do orógeno Araçuaí e norte da faixa Ribeira: geometria e significado tectônico. Ph.D Thesis. Universidade Federal de Ouro Preto, 221.

Silva T. P. de, Mello C.L, 2010, Reativações neotectônicas na zona de cisalhamento do Rio Paraíba do Sul (Sudeste do Brasil). *Revista do Instituto de Geociências*, São Paulo, 11, 1, 95-111.

Singh, K.K.K., Bharti, A.K., Pal, S.K. et al, 2019, Delineation of fracture zone for groundwater using combined inversion technique. *Environ Earth Sci,* 78, 110. https://doi.org/10.1007/s12665-019-8072-z

Singhal B.B.S., Gupta R.P, 1976, Applied hydrogeology of fractured rocks. 2nd ed. New York: Springer. 2010, 408.

Soares P. C.; Fiori A. P. Lógica e Sistemática na Análise e Interpretação de Fotografias Aéreas em Geologia. Notícia Geomorfológica, Campinas. 16, 32, 71-104.

Telford, W.M., Geldart, L.P., Sheriff, R.E. 1990. Applied Geophysics. 2ed. Cambridge: University Press. 770p.

Vieira V.S., Silva M.A. Da, Correa T.R., Lopes N.H.B, 2015, Geologia e Recursos Minerais do Estado do Estado do Espírito Santo. In: Programa Geologia do Brasil. Mapas Geológicos Estaduais, escala 1:400.000. Companhia de Pesquisa de Recursos Minerais (CPRM), Serviço Geológico do Brasil, Belo Horizonte. Brasil.

Vieira, V.S. (Org.), 1997, Programa de Levantamentos Geológicos Básicos do Brasil. Folha Cachoeiro do Itapemirim – SF.24-V-A. Estados do Espírito Santo, Minas Gerais e Rio de Janeiro, escala 1:250.000. Brasília, MME/SMM/CPRM., 99.

Yabel A., Fabro R., Guadalupe J., Ávila P., Alberich M.V.E., Sansores S.A.C. & Camargo-Valero M.A., 2015, Spatial distribution of nitrate health risk associated with groundwater use as drinking water in Merida, Mexico. *Applied Geography*, 65, 49-57. doi: 10.1016/j.apgeog.2015.10.004.

Zálan P. V., Oliveira J. A. B. de, 2005, Origem e evolução estrutural do Sistema de Riftes Cenozóicos do Sudeste do Brasil. *Boletim de Geociências da Petrobrás*. 13, 2, 269-300.